

Available online at www.sciencedirect.com

SciVerse ScienceDirect

Physics Procedia 39 (2012) 439 – 446

Physics

Procedia

LANE 2012

Mechanical properties of AlSi10Mg produced by Selective Laser Melting

K. Kempen^{a,*}, L.Thijs^b, J. Van Humbeeck^b and J.-P. Kruth^a^aUniversity of Leuven, KU Leuven, Dept. of Mech. Engineering, Celestijnenlaan 300B 3001 Leuven, Belgium^bUniversity of Leuven, KU Leuven, Dept. of Metallurgy and Mat. Engineering, Kasteelpark Arenberg 44 3001 Leuven, Belgium

Abstract

Selective Laser Melting (SLM) is an Additive Manufacturing (AM) technique in which a part is built up in a layer-by-layer manner by melting the top surface layer of a powder bed with a high intensity laser according to sliced 3D CAD data. In this work, mechanical properties like tensile strength, elongation, Young's modulus, impact toughness and hardness are investigated for SLM-produced AlSi10Mg parts, and compared to conventionally cast AlSi10Mg parts. It is shown that AlSi10Mg parts with mechanical properties comparable or even exceeding to those of conventionally cast AlSi10Mg can be produced by SLM.

© 2012 Published by Elsevier B.V. Selection and/or review under responsibility of Bayerisches Laserzentrum GmbH
Open access under [CC BY-NC-ND license](https://creativecommons.org/licenses/by-nc-nd/4.0/).

Keywords: Selective Laser Melting; AlSi10Mg; hardness; tensile strength

1. Motivation

Additive Manufacturing (AM) is a class of layer-by-layer manufacturing techniques that can fabricate highly complex components from a 3-dimensional CAD model. This model is sliced into 2D slices with a certain layer thickness, and subsequently each layer is built up by adding material.

Selective Laser Melting (SLM) is an Additive Manufacturing (AM) process where a laser source selectively scans a powder bed according to the CAD-data of the part to be produced. The high intensity laser beam makes it possible to completely melt and fuse the metal powder particles together to obtain almost fully dense parts. Successive layers of metal powder particles are melted and consolidated on top of each other resulting in near-net-shaped parts, other than surface finishing. A schematic view of the SLM process and main components of an SLM machine are illustrated in Fig. 1.

* Corresponding author. Tel.: +32-16-22552 .

E-mail address: karolien.kempen@mech.kuleuven.be .

Aluminum-Silicon alloys are characterized by sound castability, good weldability and excellent corrosion resistance. Due to their attractive combination of mechanical properties, high heat conductivity and low weight, the Al-Si alloys found a large number of applications in automotive, aerospace and domestic industries [1]. Alloying magnesium to the Al-Si alloy enables the precipitation of Mg_2Si which

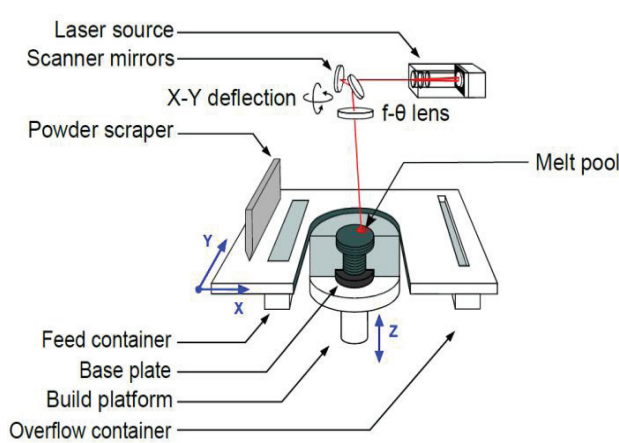


Fig. 1. Schematic overview of a SLM Machine

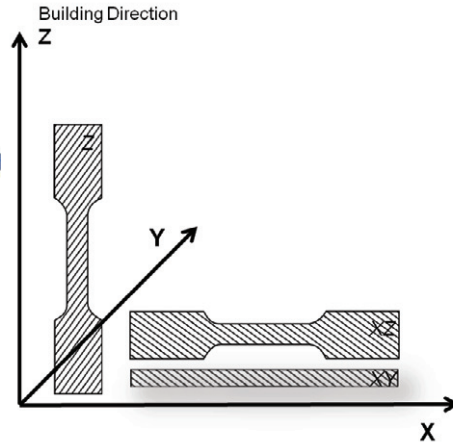


Fig. 2. Building direction of test samples

will strengthen the matrix to a significant extent without compromising the other mechanical properties. AlSi10Mg, the alloy being used in this work, contains 0.45 to 0.6 wt% Mg and can be hardened through the above mentioned precipitation mechanism by applying a specific heat treatment [2]. Furthermore, it is relatively easy to process by laser applications due to the near-eutectic composition of Al and Si which is known to lead to a small solidification range, compared to high strength aluminum alloys like the 7000 series [3].

SLM of aluminum can, due to its high geometrical freedom, offer new opportunities in applications that require complex structures and internal cavities like heat sinks [4] and lightweight structures. The immediate challenge in processing aluminum alloy powders using the SLM technique would be the high reflectivity and relatively low melting point of these powders [5,6].

2. Experimental

A modified Concept Laser M1 SLM Machine was used to process the AlSi10Mg powder. This machine can handle reactive materials in a good controlled atmosphere. It is equipped with a 200W fibre laser and has a laser beam diameter of about $150\ \mu\text{m}$ [7].

Densities were measured by comparing the weight in ethanol and air, according to the Archimedes method. Densities are expressed in %, relatively to the materials' theoretical bulk density of $2,68\text{g/cm}^3$ [source?].

Microstructures are observed under a Zeiss Axioscop 40 Pol polarizing microscope and a Philips XL30 FEG Scanning Electron Microscope.

To determine the mechanical properties, tensile, hardness and Charpy impact tests were conducted. An Instron 4505 testing machine was used for tensile testing. Hardness was measured according to the hardness Vickers scale (0,5 kg load). X-Ray diffraction patterns were measured by a Siemens D500 Goniometer.

3. Results and Discussion

In order to promote the optimum mechanical properties of AlSi10Mg parts produced by SLM, all test parts were produced using a set of parameters that result in a maximal density. The optimization of the parameters was done in a previous study [11]. Using a laser power of 200W, a scan speed of 1400mm/s and a spacing of 105 μ m between the scan tracks results in a relative density of at least 98,5%. The density can be further increased to 99,8% by re-melting every layer with the same parameters, but alternating directions over 90°.

3.1. Mechanical properties

Mechanical properties obtained from the tensile tests done on parts produced in 2 different directions (as depicted in Fig. 2), are shown in Table 1. The given values represent the mean values for 2 or 3 specimens with 95% confidence intervals. As a reference, properties for conventional casted and high pressure die casted AlSi10Mg are also shown. High pressure die casting is considered to give the optimum properties amongst the casting processes. For visualization, one stress-strain curve for each direction is shown in Fig. 3.

Table 1. Mechanical properties of SLM built parts and cast + aged parts

x \pm s	E GPa	UTS MPa	ϵ_{break} %	HV
XY direction	68 \pm 3	391 \pm 6	5,55 \pm 0,4	127
Z direction		396 \pm 8	3,47 \pm 0,6	
conventional cast and aged [8]	71	300-317	2,5-3,5	86
high pressure die casting F*[9]	71	300-350	3-5	95-105
high pressure die casting T6*[9]	71	330-365	3-5	130-133

*For the high pressure die casting AlSi10Mg parts, the properties for as-cast (F) as well as for the aged (T6) condition are given.

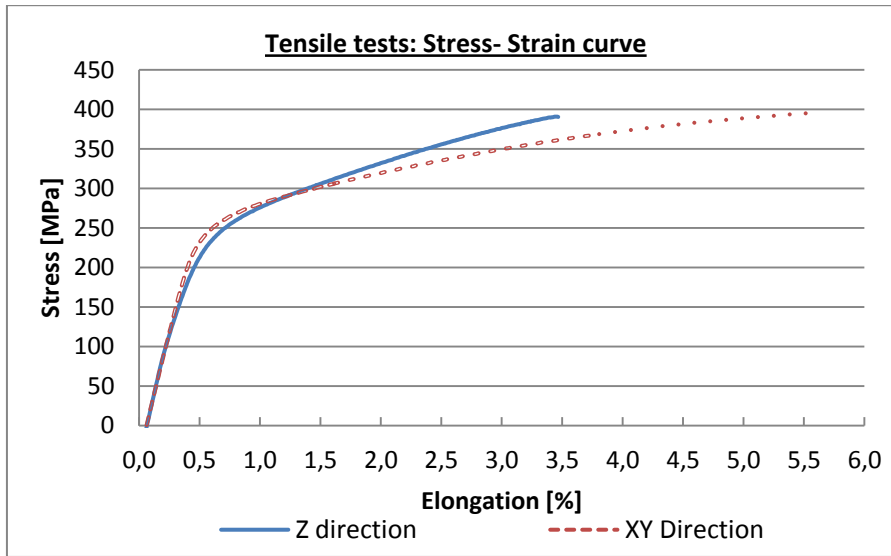


Fig. 3. Stress-Strain curve for SLM-parts produced in different directions

A first observation shows that SLM AlSi10Mg parts have mechanical properties higher or at least comparable to the casted AlSi10Mg material. The Vickers hardness of the as built SLM parts is much higher (almost 30Hv) than the hardness of the high pressure die casted (HPDC) AlSi10Mg in the as-cast condition and almost as high as the HPDC AlSi10Mg in the aged condition. The ultimate tensile strength of the as built AlSi10Mg SLM parts is always higher than those of the HPDC in both conditions. The elongation of the as-built AlSi10Mg parts in the Z-direction is comparable to the HPDC parts, while the elongation for parts built in XY – direction is almost 2% higher.

Although the strength and hardness is higher, the Charpy impact energy (Table 2) of the as-built SLM samples is still superior to that of the conventionally casted AlSi10Mg material.

Table 2. Results of Charpy impact testing

$\bar{x} \pm s$	Impact energy J
XY direction	$3,94 \pm 0,5$
Z direction	$3,69 \pm 0,48$
as-cast	2,5- 3,0

From these tensile test results, it can also be seen that the SLM samples show anisotropy in their properties. A comparison between the stress-strain curves for the two directions show a different strengthening behavior. As a result, the elongation at break is seen to be lower for the XY oriented

samples compared to the Z oriented samples. While tensile tests show a significant difference in ductility between parts produced in XY-direction and parts produced in Z-direction, this difference in ductility is not significant for Charpy test results. In tensile tests, deformation is much slower ($0.4 \text{ mm/mm min}^{-1}$) than for Charpy impact tests. Furthermore, it is interesting to notice that all samples were seen to break at UTS.

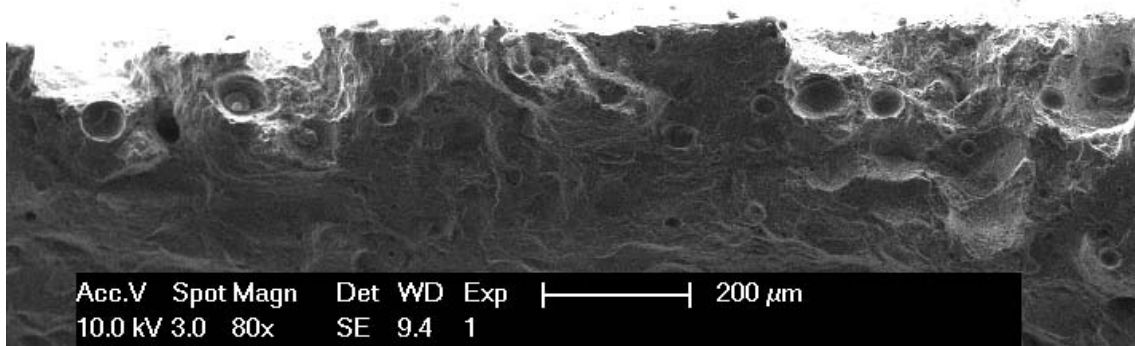


Fig. 4. Fracture Surface of a SLM-produced AlSi10Mg sample. The border of the broken test sample is shown, where the borderline porosity initiated cracks towards the side of the sample

Upon observation of the fracture surface of a tensile sample (Fig. 4), it can be seen that large pores near the border of the sample initiate the fracture. These ‘borderline pores’ are formed at the beginning/end of a scan vector. As illustrated in Fig. 5, these borderline pores are more numerous in parts produced in the Z direction, compared to parts produced in the XY direction. These pores are the largest defects present in the part. At a high stress level (i.e. 395MPa for both testing directions), they will become the critical defects which initiate inhomogeneous deformation. Because of their location close to the sample border, they lack space for extensive deformation and easily cause complete fracture of the sample. Due to the faster strengthening of the Z direction, this high stress level is reached sooner and as a result the elongation in tensile test is lower: 3,47% compared to 5,55% for XY oriented samples.

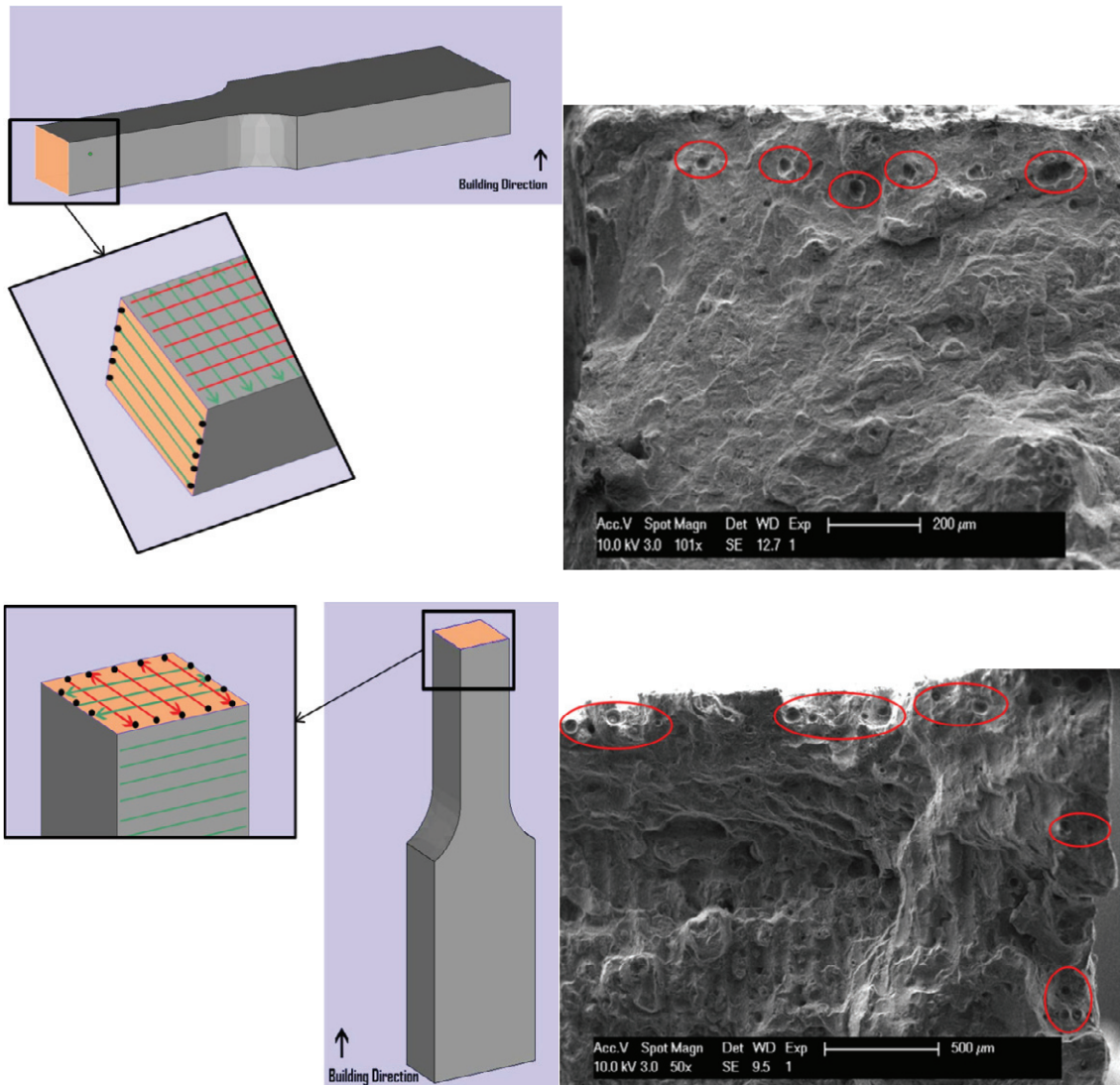


Fig. 5. a) optimal density scanning strategy for tensile samples produced in 2 directions. First zigzag scanning, then re-melting of every layer with zigzag pattern rotated over 90. Borderline pores are formed at the beginning/end of every scan vector (b) tensile sample fracture surfaces show presence of borderline porosity: in 1 direction for XY-samples (TOP image), in two directions for Z-samples (BOTTOM image)

The high hardness and strength in cast parts is reached by the formation of Mg_2Si precipitates during the heat treatment. In SLM parts, significantly higher hardness and strengths are already reached in the as-built state, i.e. non heat treated condition.. These result from the very fine microstructure and fine distribution of the Si phase in $AlSi10Mg$ SLM parts due the rapid cooling and solidification, and probably also from the presence of Mg_2Si although those precipitates were not observed by XRD analysis. The remarkably fine microstructure consisting of small Al-matrix cells/dendrites decorated with Si phase is shown in Fig. 6. [12].

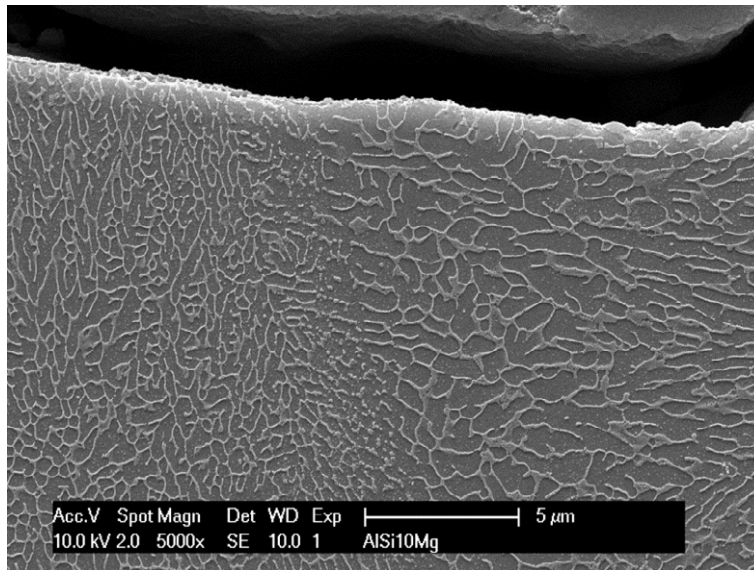


Fig. 6. SEM micrograph of a AlSi10Mg SLM part showing the Al-matrix cells decorated with Si phase. A cross section perpendicular to the layers and the scanning direction is shown here

4. Conclusions

- SLM AlSi10Mg parts have mechanical properties (Hardness, UTS, elongation, impact energy) higher or at least comparable to the casted AlSi10Mg material, because of the very fine microstructure and fine distribution of the Si phase
- SLM samples show some anisotropy in elongation at break. This is because of the optimal density scanning strategy which causes Z-oriented tensile samples to form more borderline porosity. These pores make the Z-oriented tensile parts more sensitive to crack initiation, compared to XY-oriented tensile samples.

References

- [1] Vilaro, T. et al. Direct manufacturing of technical parts using selective laser melting: example of automotive application. In: *Proc. of 12th European Forum on Rapid Prototyping*, 2008, France.
- [2] ASM Handbook, Volume 2 Properties and Selection: nonferrous alloys and special-purpose materials, 1990, ASM International The Materials Information Company, United States of America, ISBN 0-87170-379-3, pp.3-14.
- [3] Louvis, E., Fox, P. and Sutcliffe, J. Selective laser melting of aluminium components, *Journal of Materials Processing Technology* **211** (2011), pp. 275–284.
- [4] Wong, M., Tsoupanos, S., Sutcliffe, C.J. and Owen, I. Selective laser melting of heat transfer devices, *Rapid Prototyping Journal* **13** (5) (2007), pp. 291–297.
- [5] Voncina, M., Mrvar, P. and Medved, J. Thermodynamic analysis of AlSi10Mg alloy. *RMZ Materials and Geoenvironment*, **52** (3) (2006), pp. 621–633.
- [6] Buchbinder, D., Schleifenbaum, H., Heidrich, S., Meiners, W. and Bültmann, J. High power selective laser melting (HP SLM) of Aluminium parts. *Physics Procedia* **12** (1) (2011), pp. 271–278.

- [7] Concept Laser GmbH/ M1, Web-Based Data, Concept Laser GmbH Co., Germany, <http://www.concept-laser.de/>, as on 04.05.2012.
- [8] Matweb materials data, Web-Based Data, Matweb, UK <http://www.matweb.com/>, as on 04.05.2012.
- [9] Flagship Technical data sheets for heat treated aluminium high pressure die castings.
- [10] Wong, T.T., Liang, G.Y., Tang, C.Y. The surface character and substructure of aluminium alloys by laser-melting treatment. *Journal of Materials Processing Technology* **66** (1–3) (1997), pp. 172–178.
- [11] Kempen, K., Thijs, L., Yasa, E., Badrossamay, M., Verheecke, W., Kruth, J. (2011). Microstructural analysis and process optimization for selective laser melting of AlSi10Mg. *Solid Freeform Fabrication Symposium Proceedings*. Solid Freeform Fabrication Symposium. Austin, Texas, USA, 8-10 August 2011.
- [12] Thijs, L., Kempen, K., Kruth, J.-P., Van Humbeeck, J. Influence of scanning strategy on the microstructure and texture of Selective Laser Melted AlSi10Mg products (*in preparation*).